Mechanical and Morphological Properties of Lyocell Blends: Comparison with Lyocell Nanocomposites (I)

Jin-Hae Chang, Si Wook Nam, Seo-Won Jang

Department of Polymer Science and Engineering, Kumoh National Institute of Technology, Gumi 730-701, Korea

Received 5 July 2006; accepted 6 May 2007
DOI 10.1002/app.26845
Published online 9 August 2007 in Wiley InterScience (www.interscience.wiley.com).

ABSTRACT: The mechanical properties and morphologies of polyblends of lyocell with three different fillers are compared. Poly(vinyl alcohol) (PVA), poly(vinyl alcohol-*co*-ethylene) (EVOH), and poly(acrylic acid-*co*-maleic acid) (PAM) were used as fillers in blends with lyocell produced through solution blending. The variations of their properties with polymer matrix filler content are discussed. The ultimate tensile strength of the PVA/lyocell blend is highest for a blend lyocell content of 30 wt %, and decreases as the lyocell content is increased up to 40 wt %. The ultimate tensile strengths of the EVOH/lyocell and PAM/lyocell blends are highest for a lyocell loading of 20 wt %, and decrease with the increasing filler content. The variations in the initial moduli of the blends with filler content are similar. Of the three blend systems, the blends with PVA exhibit the best tensile properties. Lyocell/organoclay hybrid films were prepared by the solution intercalation method, using dodecyltriphenylphosphonium–Mica (C_{12}PPh-Mica) as the organoclay. The variation of the mechanical tensile properties of the hybrids with the matrix polymer organoclay content was examined. These properties were found to be optimal for an organoclay content of up to 5 wt %. Even polymers with low organoclay contents exhibited better mechanical properties than pure lyocell. The addition of organoclay to lyocell to produce nanocomposite films was found to be less effective in improving its ultimate tensile strength than blending lyocell with the polymers. However, the initial moduli of the nanocomposites were found to be higher than those of the polyblend films. © 2007 Wiley Periodicals, Inc. J Appl Polym Sci 106: 2970–2977, 2007

Key words: lyocell; blend; organoclay; nanocomposite; film

INTRODUCTION

Conventional plastics are generally fabricated from petroleum-based polymers and their large-scale consumption has generated serious environmental problems. As a result, much attention has recently been devoted to the development of biodegradable and environmentally friendly polymers.[1–4]

Solvent-spun cellulose fiber, lyocell, was first investigated in the early 1980s, partly to improve the environmental acceptability of the well-established viscose process.[5,6] Lyocell is an environmentally benign man-made fiber, because lyocell is manufactured by dissolving cellulose in *N*-methyl morpholine-*N*-oxide monohydrate (NMMO). The manufacturing process is designed to recover 99% of the solvent, which minimizes effluent. The solvent itself is nontoxic, and all the effluent is nonhazardous.[7–11]

Composite materials can have excellent mechanical and thermal properties, and so are widely used in various applications ranging from aerospace materials to vehicles to sports equipment. To improve the properties of composites, crosslinking, H-bonding, and transesterification between multifunctional groups in the polymer chains have been used, in particular, between hydroxyl and carboxyl groups.[12–16] For example, PVA and EVOH are more tightly bound in composites where hydrogen-bonding (H-bonding) occurs between fillers and polymeric chains. As a result, composite materials with H bonds can exhibit better properties than those of pure polymers.

Nanoscaled composites of polymers with organoclays have been studied extensively.[17–20] Nanostructured materials often possess a combination of physical and mechanical properties not present in conventional polymer matrix composites. Even at low clay contents (<10 wt %), the strength and modulus of the polymer matrix can be substantially increased.[21–26]

The main objective of this study was to investigate the variations in the mechanical properties and morphologies with the polymer filler content of the lyocell matrix. As fillers, we used PVA and EVOH (containing hydroxyl groups) and PAM (containing carboxyl groups). The introduction of hydroxyl and carboxyl groups into the lyocell matrix, which contains HO-groups, modifies the lyocell chemical structure because of the formation of H bonds. In particular, PAM is a crosslinking agent and a donor of the hydrophilic —COOH group. This work also investigates the effects of the addition of an organoclay to

Correspondence to: J.-H. Chang (changjinhae@hanmail.net).
Contract grant sponsor: Korea Institute of Industrial Technology (KITECH); contract grant number: 2005-33.

Journal of Applied Polymer Science, Vol. 106, 2970–2977 (2007)

lyocell on its mechanical properties. The variations in the properties of the nanocomposites in film form with matrix polymer clay content were studied. Furthermore, we compare the mechanical and morphological properties of the two different lyocell composites.

EXPERIMENTAL

Materials

Lyocell and NMMO were kindly supplied by Kolon, Seoul, Korea. The PVA (99.3–99.7% hydrolyzed, average Mw = 74,800; Dupont) used in this study was purchased from Dupont, Seoul, Korea. EVOH (ethylene content 27 mol %; Aldrich) and PAM (50 wt % solution in water, Mw = 3,000; Aldrich) were purchased from Aldrich Chemical, Seoul, Korea. The water used was distilled and deionized. Common reagents were used without further purification.

Preparation of the organoclay: C_{12}PPh-Mica

The organically modified clay (C_{12}PPh-Mica) used in this study was synthesized via the ion exchange reaction between Na^+-mica and dodecyltriphenylphosphonium chloride (C_{12}PPh-Cl^-) with the method described in our previous study.[27] The chemical structure of C_{12}PPh-Mica is as shown:

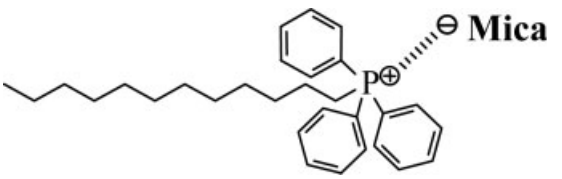

Preparation of the lyocell blend films

It is well known that lyocell does not melt, but instead exhibits thermal degradation at high temperatures. Therefore, to produce lyocell films, it must be dissolved in NMMO.[7,11] NMMO also have shown sufficient solvating ability for PVA, EVOH, and PAM. Since the synthetic procedures used for the lyocell blend films with the three different fillers were very similar, only the preparation of the 30% PVA/lyocell blend film is described here. The polymer concentration in NMMO (72 g) was kept at 4 wt % (3 g) (2.1 g of lyocell + 0.9 g of PVA) to guarantee uniform mixing. The polymer solution was mixed with vigorous agitation for 2 h at 115°C under a steady stream of N_2 gas, and the resulting blend solution was cast onto a glass plate. The solvent was removed in a water bath for 1–2 h. The films were dried in a drying oven at 30°C for 1 day. The resulting film thickness was 10–15 μm.

Preparation of the C_{12}PPh-Mica/lyocell nanocomposite films

All of the samples were prepared as solutions. Since the syntheses of the nanocomposite films were very similar, only a representative example, the procedure for the preparation of the nanocomposite containing 3 wt % organoclay, is described here. About 29.1 g of lyocell and 0.9 g of C_{12}PPh-Mica were placed in a three-necked flask, and the mixture was stirred for 2 h at 115°C under a steady stream of N_2 gas. Mechanical stirring was used to obtain a homogeneously dispersed system. This mixture was cast onto a glass plate. The glass plate was soaked in a water bath to remove NMMO for 1–2 h. The films were dried in a drying oven at 30°C for 1 day. The resulting film thickness was 10–15 μm.

Characterization

Wide-angle X-ray diffraction (WAXD) measurements were performed at room temperature with an X'Pert PRO-MRD X-ray diffractometer using Ni-filtered Cu Kα radiation. The scanning rate was 2°/min over ranges of 2θ = 2°–32° for the blend films and 2θ = 2° – 12° for the nanocomposite films.

The tensile properties of the films were determined at room temperature using an Instron mechanical tester (Model 5564) at a crosshead speed of 20 mm/min. The experimental uncertainties in the tensile strengths and moduli were ±1 MPa and ±0.05 GPa respectively. These properties were determined from the average of at least 10 individual determinations.

The morphologies of the fractured film surfaces were investigated using SEM (model S-2400, Hitachi). An SPI sputter coater was used to sputter the fractured surfaces with gold so as to enhance their conductivity. The samples were prepared for transmission electron microscopy (TEM) by placing the lyocell nanocomposite films into epoxy capsules and then curing the epoxy at 70°C for 24 h in vacuum. The cured epoxies containing the lyocell nanocomposites were then microtomed into 90-nm thick slices, and a layer of carbon, about 3 nm thick, was deposited onto each slice on a mesh 200 copper net. TEM photographs of ultrathin sections of the polymer/organoclay nanocomposite samples were obtained with an EM 912 OMEGA transmission electron microscope using an acceleration voltage of 120 kV.

RESULTS AND DISCUSSION

Dispersion of the blended films

Figure 1 shows the XRD curves of EVOH, PVA, PAM, and lyocell for the range 2θ = 2°–32°. The curves have peaks corresponding to basal spacings

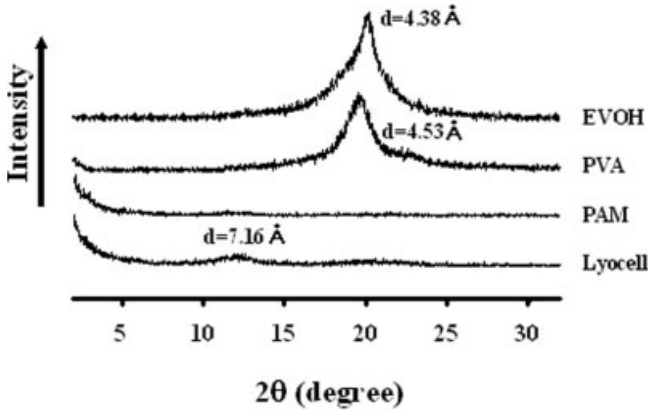

Figure 1 XRD patterns of lyocell, PVA, EVOH, and PAM.

of 4.38 Å for EVOH and 4.53 Å for PVA. In the case of lyocell, a very small peak was observed at $2\theta = 12.35^\circ$, corresponding to an interlayer distance of 7.16 Å. The XRD curve of PAM does not contain peaks, which indicate an amorphous structure.

Figure 2 shows the XRD curves of films of lyocell, PVA, and lyocell blends with various PVA contents. The curves of pure lyocell and pure PVA contain their characteristic peaks. The curves of the blends with PVA content in the range 10–40 wt % contain a very small peak, at $2\theta = 12.35^\circ$ ($d = 7.16$ Å), which is the same as the peaks of lyocell. The intensities of the XRD peaks are almost the same for PVA loadings up to 40 wt %. However, there is an additional a very small peak at $2\theta = 6.31^\circ$ ($d = 13.99$ Å). The presence of this peak is an indication that PVA is not dispersed homogeneously in the lyocell matrix. It also suggests that the dispersion is better at a lower PVA loading than at a higher PVA loading. Similar XRD results were obtained for the EVOH and PAM polymer blend films (not shown here).

The PVA dispersion in the lyocell matrix was determined with electron microscopy. Electron microscopy and XRD can be used as complementary techniques to fill in the gaps in information provided by other techniques.[28–30] The morphologies of the films containing up to 40 wt % PVA in a lyocell matrix were examined by observing their fracture surfaces with SEM, and the results are shown in Figure 3.

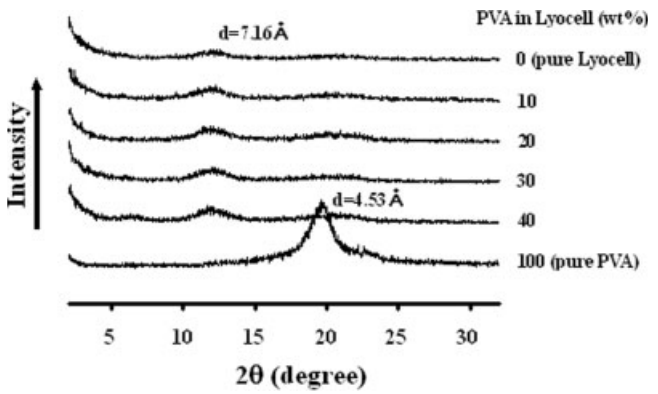

Figure 2 XRD patterns of lyocell blend films with various PVA contents.

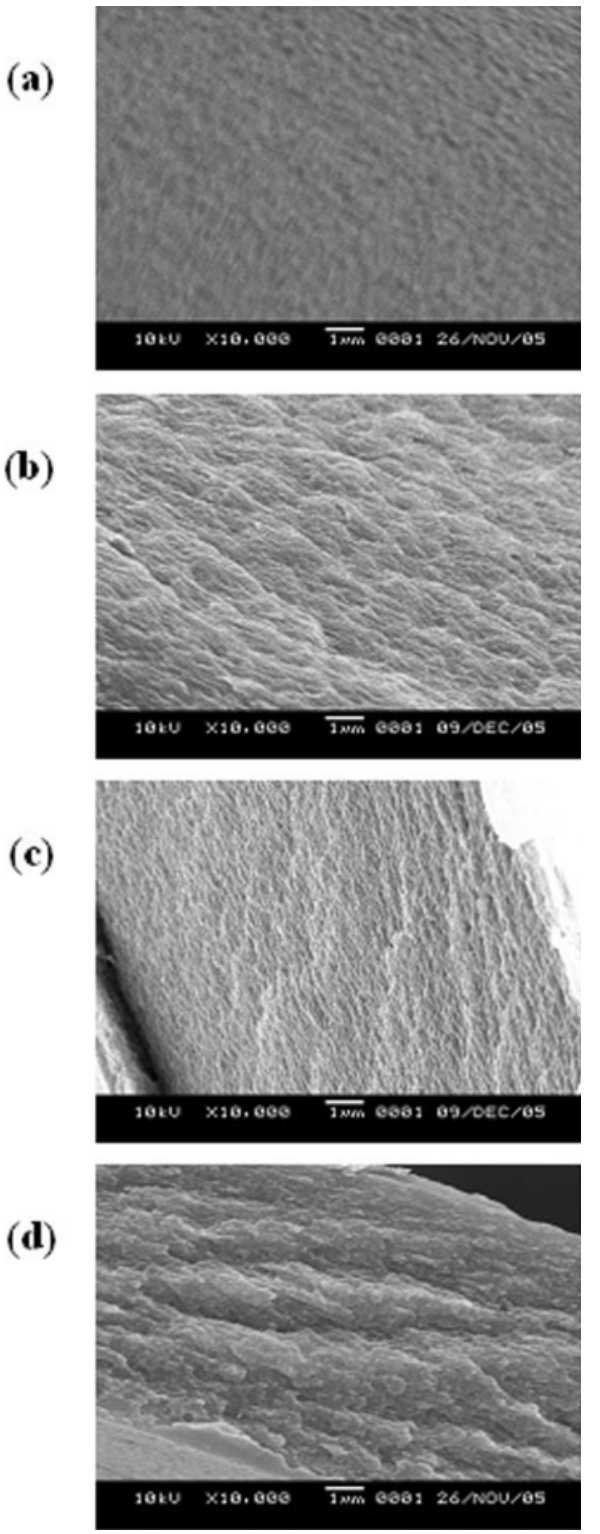

Figure 3 SEM photographs of lyocell blend films with various PVA contents: (a) 0 wt % (pure lyocell), (b) 10 wt %, (c) 30 wt %, and (d) 40 wt %.

TABLE I
Mechanical Tensile Properties of the Lyocell Blend Films

	Ult. Str. (MPa)			Ini. Mod. (GPa)			E. B.[b] (%)		
Blend[a] (wt %)	PVA	EVOH	PAM	PVA	EVOH	PAM	PVA	EVOH	PAM
0 (Pure lyocell)	42	42	42	4.18	4.18	4.18	5	5	5
10	60	52	60	4.76	4.43	4.22	5	2	2
20	62	70	63	4.79	5.31	5.17	6	3	2
30	74	50	59	5.50	3.70	4.21	7	3	3
40	49			3.92			9		

[a] Filler contents of the lyocell blend films.
[b] Elongation percent at break.

The lyocell blend films with 0–30 wt % PVA are well dispersed in a continuous lyocell phase [see Fig. 3(a–c)]. Above 40 wt % of PVA, more fractured deformation surfaces were found in Figure 3(d). This is probably a consequence of some agglomeration of the polymer particles, which is consistent with the XRD observations shown in Figure 2.

Tensile properties of the blend films

The mechanical tensile properties of lyocell blend films with various filler contents are shown in Table I. The strength and modulus values were found to be enhanced remarkably in comparison to those of lyocell for filler contents up to a critical content, with decreases above that content. It appears that there is a critical amount of filler beyond which the filler's reinforcing capacity diminishes. For example, in Table I, the strength of the 30 wt % PVA blend film is shown to be 74 MPa, which is about 70% higher than that of pure lyocell (42 MPa). When the PVA content is 40 wt %, the strength is 49 MPa. This decrease in the ultimate tensile strength is mainly due to the agglomeration of filler particles above a critical PVA content. This was confirmed by carrying out morphological studies with SEM [see Fig. 3(d)]. In short, the reinforcing effect does not obey a rule of mixtures in this blend system. Similar results have previously been obtained with other polymer blends.[31–33] For filler contents of 20 wt %, the strengths of the EVOH and PAM blends are at their maximum values.

A similar trend was observed for the initial modulus. The initial modulus of the PVA/lyocell blend films increases with the addition of PVA up to a critical PVA loading and then decreases above that critical content; the value of the initial modulus increases from 4.18 to 5.50 GPa with increases in the PVA content up to 30 wt % and is 3.92 GPa for 40 wt % PVA content. Similar results were also obtained for the EVOH and PAM blends; when the amount of filler in lyocell is 20 wt %, the initial moduli of these polyblend films are at their maximum values. The ultimate strength and initial modulus of the PVA blends are the best of those of the three blend systems: the 30 wt % PVA/lyocell blend film has a strength of 74 MPa and an initial modulus of 5.50 GPa. It is suggested that the hydroxyl groups (—OH) in PVA provide strong H-bonding between the filler polymer and the substrate, and that its polymer main chains maintain the polyblend's rigidity. A combination of these two factors produces the remarkable reinforcing effects found for PVA. The variations of the ultimate strength and the initial modulus with filler content are shown in Figures 4 and 5, respectively.

The elongation percent at break (EB) values were found to increase linearly with increase in the organoclay content of the PVA blends. When the PVA content was increased to 40 wt %, the EB of the blend film was found to be 9%, about twice as great as that of pure lyocell (5%). It seems that H-bonding interactions elevate the interfacial adhesion between PVA and lyocell. The EB values of the other two systems were found to decrease from 5 to 2% with this increase in filler content and are then constant with further increase in the filler content (see Fig. 6).

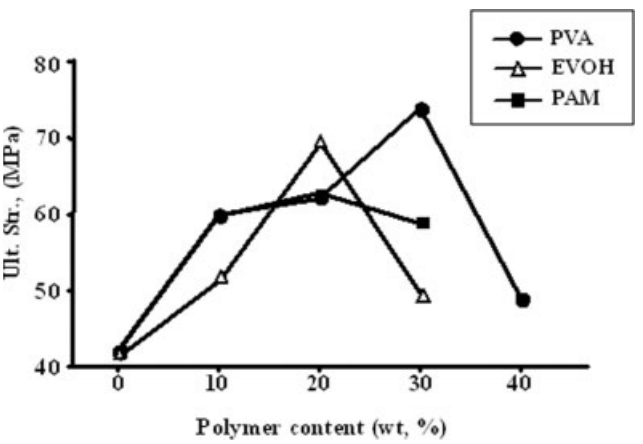

Figure 4 Effects of PVA content on the ultimate tensile strength of the lyocell blend films.

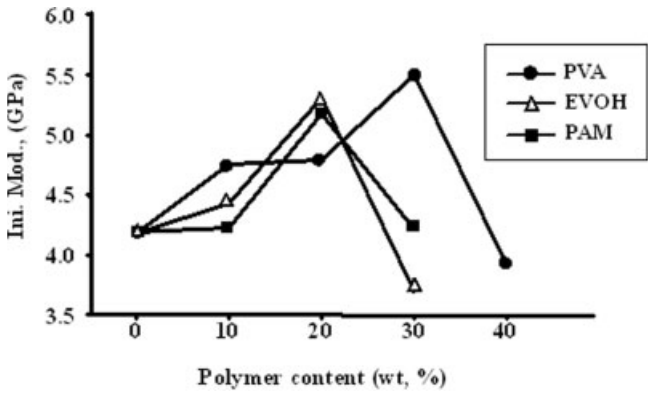

Figure 5 Effects of PVA content on the initial tensile modulus of the lyocell blend films.

Dispersion of the organoclay in the nanocomposites

The XRD results for the C_{12}PPh-Mica/lyocell nanocomposite films are shown in Figure 7. The d_{001} reflection in Na^+-mica was found at $2\theta = 9.23^\circ$, which corresponds to an interlayer distance of 9.57 Å. The XRD peak for the surface-modified clay, C_{12}PPh-Mica, was found at $2\theta = 3.15^\circ$, corresponding to an interlayer distance of 28.01 Å. As expected, the ion exchange between Na^+-mica and dodecyltriphenylphosphonium chloride (C_{12}PPh-Cl^-) results in an increase in its basal interlayer spacing over that of pristine Na^+-mica, and results in a big shift of the diffraction peak toward lower values of 2θ.[34] This increased spacing also leads to easier dissociation of the clay, resulting in hybrids with better clay dispersion.[35,36]

Only a slight peak at d = 14.94 Å was found in the XRD results for the lyocell films with 1 wt % organoclay content (see Fig. 7). Substantial increase in the intensities of the XRD peaks was observed for increases in the clay loading from 1 to 7 wt %, which suggests that the dispersion is more effective at a lower clay loading than at a higher clay loading. Higher clay loadings are expected to result in easier agglomeration within the lyocell matrix of some portion of the clay.

The presence of the organoclay was found, however, to have no effect on the location of the peak, which indicates that the exfoliation of the clay layer structure of the organoclay does not occur in lyocell.[30] The disappearance of the main peak at $2\theta = 3.15^\circ$ for the lyocell nanocomposites occurs because the peak of the swollen organoclay inserted into the polymer chains is below 2°.

Morphologies of the nanocomposites

Although XRD is by far the simplest method available for measuring the d spacing of nanocomposites, SEM and TEM were also used to evaluate the degree of intercalation and the amount of aggregation in the clay clusters. The morphology of the aggregated clay can be characterized using SEM. Because of the difference between the scattering densities of clay and lyocell, large clay aggregates can easily be imaged with SEM.

The SEM images of the fractured surfaces of the lyocell nanocomposite films containing the various organoclays are compared in Figure 8. The morphologies of the nanocomposite films containing up to 7 wt % C_{12}PPh-Mica in the lyocell matrix were examined by observing their fracture surfaces with SEM. The lyocell nanocomposite films with 3–5 wt % C_{12}PPh-Mica [Fig. 8(b,c)] contain uniform and disperse phases. In contrast, the film containing 7 wt % organoclay [Fig. 8(d)] contains voids and some deformed regions that may result from the coarseness of the fractured surface. The fractured surfaces were found to be more deformed for higher hybrid

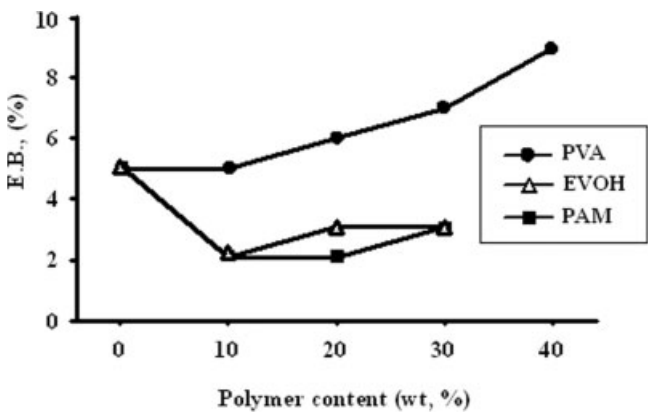

Figure 6 Effects of PVA content on the elongation percent at break of the lyocell blend films.

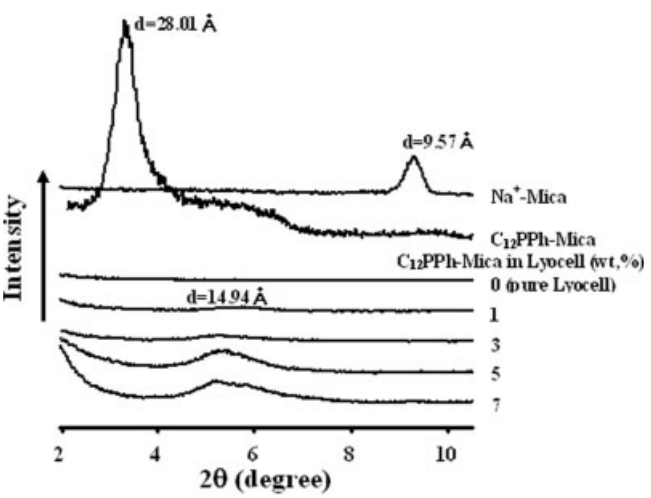

Figure 7 XRD patterns of clay, organoclay, and lyocell nanocomposite films with various organoclay contents.

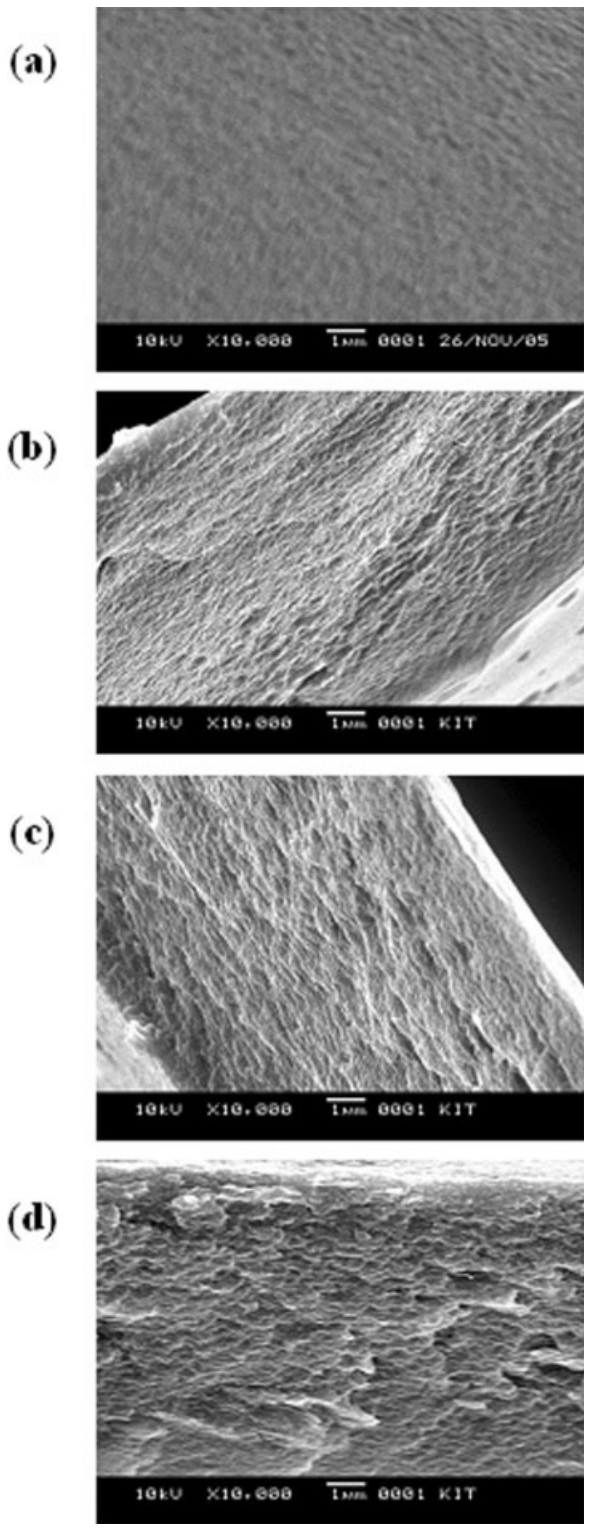

Figure 8 SEM photographs of lyocell nanocomposite films with various C_{12}PPh-Mica contents (a) 0 wt % (pure lyocell), (b) 3 wt %, (c) 5 wt %, and (d) 7 wt %.

organoclay contents. This is probably a consequence of the agglomeration of clay particles. This result appears to be related to the lack of interfacial interactions between the clay and the matrix polymers; thus, many defects and agglomerations occur in interphase areas. Similar trends have been observed in studies of other polymer hybrids.[35,37,38]

More direct evidence for the formation of a true nanoscaled composite was provided by the TEM analysis of an ultramicrotomed section. TEM can provide a qualitative understanding of internal structures through direct observation. Typical TEM photographs for nanocomposite films with 5 wt % C_{12}PPh-Mica are shown in Figure 9. The dark lines are the intersections of 1-nm thick sheet layers. Figure 9(a,b) shows that the organoclay is dispersed in the polymer matrix at all magnification levels, although some parts are agglomerated at size levels greater than $\sim$ 10 nm. The presence of peaks in the XRD patterns of these samples is attributed to these agglomerated layers (see Fig. 7).

For low clay contents, clay particles may be better dispersed in matrix polymers without significant agglomeration of particles than they are for high clay contents.[37] However, agglomerated structures form and become denser in the lyocell matrix above a clay content of 7 wt %. This is consistent with the XRD results shown in Figure 7.

Tensile properties of the nanocomposite films

The tensile mechanical properties of pure lyocell and its nanocomposite films are listed in Table II. The ultimate strength and initial modulus of the lyocell nanocomposite films increase with the addition of clay up to a critical clay loading, and then decrease above that critical content. For example, the strength and modulus of the lyocell nanocomposite films are greatest at 5 wt %, 53 MPa, and 6.09 GPa, respectively. These enhancements of the tensile properties of lyocell are ascribed to the resistance exerted by the clay itself, as well as to the orientation and aspect ratio of the clay layers. When the amount of organoclay is increased from 5 to 7 wt %, the strength and modulus decrease simultaneously, as shown in Table II. The variations of the ultimate strength and the initial modulus with clay content are shown in Figure 10.

TABLE II
Mechanical Tensile Properties of the Lyocell Nanocomposite Films

Clay (wt %)	Ult. Str. (MPa)	Ini. Mod. (GPa)	E. B.[a] (%)
0 (Pure lyocell)	42	4.18	5
1	41	5.18	5
3	42	5.27	4
5	53	6.09	5
7	50	4.13	5

[a] Elongation percent at break.

The strength values of the blend films were found to be superior to those of the nanocomposite films (see Table I). This suggests that the hydroxyl groups result in the formation of H-bonds between the filler polymer and the lyocell matrix, and that this H-bonding interaction significantly improves the interfacial adhesion. This factor seems to be the major reason for the remarkable reinforcing effects of blending on the tensile properties. However, the initial moduli of the nanocomposite films are higher than those of the blend films because of the stiffness of the clay as well as the orientation and high aspect ratio of the clay layers.

The elongation at breakage of the nanocomposite films was found to be virtually unchanged by variation in the organoclay content, i.e., it changed from 4 to 5% as the organoclay content was increased from 0 to 7 wt %. This result is characteristic of materials reinforced with stiff inorganic materials and is indicative of an intercalated morphology.

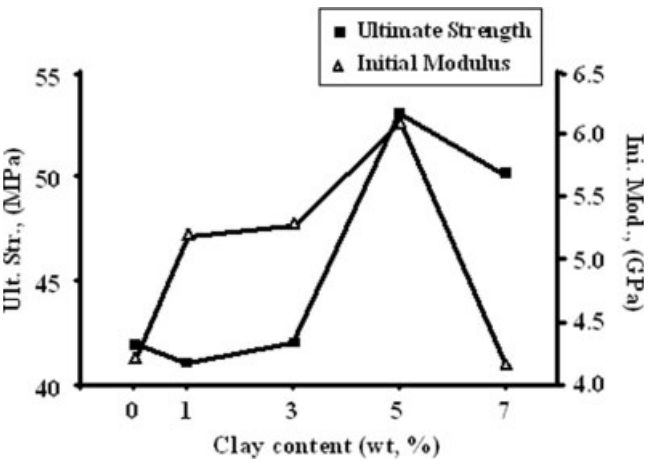

Figure 10 Effect of organoclay content on the mechanical tensile properties of the lyocell nanocomposite films.

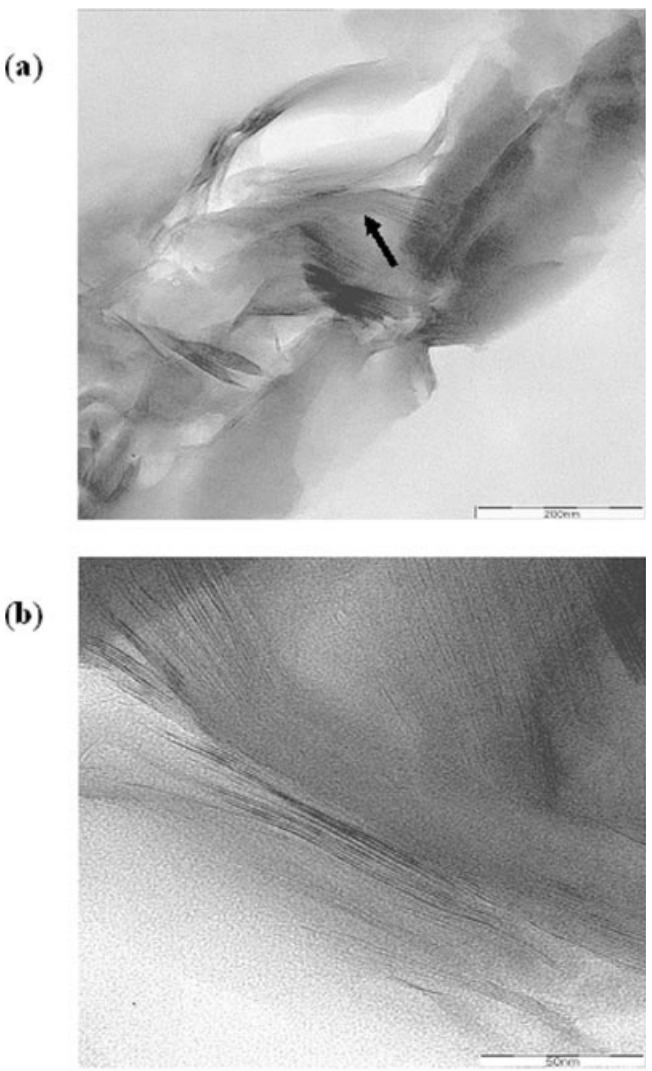

Figure 9 TEM micrographs of lyocell nanocomposite films with 5 wt % C_{12}PPh-Mica, with an increase in the magnification level from (a) to (b).

CONCLUSIONS

In this study, we have tried to clarify the effects in the film state of reinforcing lyocell with filler polymers. We demonstrated that when the fillers are properly selected, the tensile properties of the blend films are better than those of lyocell by 20–75%. Among the three tested fillers, we found that the addition of PVA produced the blend films with the best mechanical properties. We conclude that H-bonding enhances the adhesion between the filler and the lyocell matrix. This interfacial adhesion means that, of the three fillers examined in this study, PVA is the best reinforcing component.

The addition of an organoclay to lyocell to form nanocomposite films was also found to enhance the initial tensile modulus, because of the rigidity and stiffness of the clay, but is less effective in improving the ultimate tensile strength, particularly in comparison with results achieved for the conventional polyblend films. The ultimate strength and initial modulus of the blends and nanocomposites increase with the addition of filler up to a critical loading, and then decrease above that critical content.

The morphological studies indicate that the dispersion in the lyocell matrix is better at a lower filler loading than at a higher filler loading. For low clay contents, the filler particles are better dispersed in the matrix polymer without significant agglomeration of particles. Such agglomeration of filler particles in the matrix polymer results in inferior mechanical properties.

References

1. Ikeda, Y.; Tsuji, H. Macromol Rapid Commun 2000, 21, 117.
2. Okada, M. Prog Polym Sci 2002, 27, 87.
3. Kanie, O.; Tanaka, A.; Mayumi, T.; Kitaoka, T.; Wariishi, H. J Appl Polym Sci 2005, 96, 861.
4. Saheb, D. N.; Jog, J. P. Adv Polym Technol 1999, 18, 351.
5. Franks, N. E.; Varga, J. K. (to Akzona Inc.). U.S. Pat. 4,145,532.
6. Franks, N. E.; Varga, J. K. (to Akzona Inc.). U.S. Pat. 4,196,282.
7. Patrick, W. M. In Regenerated Cellulose Fibers; Woodings, C., Ed.; CRC Press: Cambridge, UK, 2001; Chapter 4.
8. Kim, B. C. Polym Sci Tech 1997, 8, 573.
9. Chanzy, H.; Peguy, S.; Chaunis, S.; Monzie, P. J Polym Sci Part B: Polym Phys 1980, 18, 1137.
10. Thomas, R.; Antje, P.; Herbert, S.; Paul, K. Prog Polym Sci 2001, 26, 1763.
11. Woodings, C. R. Int J Biol Macromol 1995, 17, 305.
12. Rhim, J. W.; Hwang, H. S.; Kim, D. S.; Park, H. B.; Lee, C. H.; Lee, Y. M.; Moon, G. Y.; Nam, S. Y. Macromol Res 2005, 13, 135.
13. Nam, S. Y.; Sung, K. S.; Chon, S. W.; Rhim, J. W. Membr J 2002, 12, 255.
14. Chang, J.-H.; Jang, T.-G.; Ihn, K. J.; Lee, W.-K.; Sur, G. S. J Appl Polym Sci 2003, 90, 3208.
15. Yeun, J.-H.; Bang, G.-S.; Park, B. J.; Ham, S. K.; Chang, J.-H. J Appl Polym Sci 2006, 101, 591.
16. Grunlan, J. C.; Grigorian, A.; Hamilton, C. B.; Mehrabi, A. R. J Appl Polym Sci 2003, 90, 3208.
17. Liang, Z.-M.; Yin, J. J Appl Polym Sci 2003, 90, 1857.
18. Ishida, H.; Campbell, S.; Blackwell, J. Chem Mater 2000, 12, 1260.
19. Itagaki, T.; Komori, Y.; Kuroda, K. J Mater Chem 2001, 11, 3291.
20. Yano, K.; Usuki, A.; Okada, A. J Polym Sci Part A: Polym Chem 1997, 35, 2289.
21. Lan, T.; Pinnavaia, T. J. Chem Mater 1994, 6, 2216.
22. Osman, M. A.; Mittal, V.; Morbidelli, M.; Suter, U. W. Macromolecules 2003, 36, 9851.
23. Bharadwaj, R. K. Macromolecules 2001, 34, 9189.
24. Liang, Z.-M.; Yin, J. J Appl Polym Sci 2003, 90, 1857.
25. Ishida, H.; Campbell, S.; Blackwell, J. Chem Mater 2000, 12, 1260.
26. Itagaki, T.; Komori, Y.; Kuroda, K. J Mater Chem 2001, 11, 3291.
27. Chang, J.-H.; Kim, S. J.; Joo Y. L; Im, S. Polymer 2004, 45, 919.
28. Vaia, R. A.; Jandt, K. D.; Kramer, E. J.; Giannelis, E. P. Chem Mater 1996, 8, 2628.
29. Galgali, G.; Ramesh, C.; Lele, A. Macromolecules 2001, 34, 852.
30. Morgan, A. B.; Gilman, J. W. J Appl Polym Sci 2003, 87, 1329.
31. De Meuse, M. T.; Jaffe, M. Mol Cryst Liq Cryst 1988, 157, 535.
32. De Meuse, M. T.; Jaffe, M. Polm Adv Technol 1990, 1, 81.
33. Chang, J.-H.; Jo, B.-W. J Appl Polym Sci 1996, 60, 939.
34. Ke, Y.; Lu, J.; Yi, X.; Zhao, J.; Qi, Z. J Appl Polym Sci 2000, 78, 808.
35. Zilig, C.; Mulhaupt, R.; Finter, J. Macromol Chem Phys 1999, 200, 661.
36. Danumah, C.; Bousmina, M.; Kaliaguine, S. Macromolecules 2003, 36, 8208.
37. Chang, J.-H.; Park, D. K.; Ihn, K. J. J Polym Sci Part B: Polym Phys 2001, 39, 471.
38. Yang, F.; Qu, Y.; Yu, Z. J Appl Polym Sci 1998, 69, 355.